Acta Psychiatrica Scandinavica

Acta Psychiatr Scand 2017: 136: 623–636

DOI: 10.1111/acps.12824

Neurobiological support to the diagnosis of ADHD in stimulant-naïve adults: pattern recognition analyses of MRI data

Chaim-Avancini TM, Doshi J, Zanetti MV, Erus G, Silva MA, Duran FLS, Cavallet M, Serpa MH, Caetano SC, Louza MR, Davatzikos C, Busatto GF. Neurobiological support to the diagnosis of ADHD in stimulant-naïve adults: pattern recognition analyses of MRI data.

Objective: In adulthood, the diagnosis of attention-deficit/hyperactivity disorder (ADHD) has been subject of recent controversy. We searched for a neuroanatomical signature associated with ADHD spectrum symptoms in adults by applying, for the first time, machine learning-based pattern classification methods to structural MRI and diffusion tensor imaging (DTI) data obtained from stimulant-naïve adults with childhood-onset ADHD and healthy controls (HC).
Method: Sixty-seven ADHD patients and 66 HC underwent high-resolution T1-weighted and DTI acquisitions. A support vector machine (SVM) classifier with a non-linear kernel was applied on multimodal image features extracted on regions of interest placed across the whole brain.
Results: The discrimination between a mixed-gender ADHD subgroup and individually matched HC (n = 58 each) yielded area-under-the-curve (AUC) and diagnostic accuracy (DA) values of up to 0.71% and 66% (P = 0.003) respectively. AUC and DA values increased to 0.74% and 74% (P = 0.0001) when analyses were restricted to males (52 ADHD vs. 44 HC).
Conclusion: Although not at the level of clinically definitive DA, the neuroanatomical signature identified herein may provide additional, objective information that could influence treatment decisions in adults with ADHD spectrum symptoms.

T. M. Chaim-Avancini[1,2], J. Doshi[3], M. V. Zanetti[1,2], G. Erus[3], M. A. Silva[4], F. L. S. Duran[1,2], M. Cavallet[1,2], M. H. Serpa[1,2], S. C. Caetano[5], M. R. Louza[4], C. Davatzikos[3], G. F. Busatto[1,2]

[1]Laboratory of Psychiatric Neuroimaging (LIM-21), Department and Institute of Psychiatry, Faculty of Medicine, University of São Paulo, Sao Paulo, [2]Center for Interdisciplinary Research on Applied Neurosciences (NAPNA), University of São Paulo, Sao Paulo, Brazil, [3]Section of Biomedical Image Analysis, Department of Radiology, University of Pennsylvania, Philadelphia, PA, USA, [4]Program for Attention Deficit Hyperactivity Disorder (PRODATH), Department and Institute of Psychiatry, Faculty of Medicine, University of São Paulo, Sao Paulo and [5]Department of Psychiatry, Child and Adolescent Psychiatry Unit (UPIA), Universidade Federal de São Paulo, São Paulo, Brazil

Key words: attention-deficit/hyperactivity disorder; adults; structural MRI; diffusion tensor imaging; machine learning-based methods

Tiffany M. Chaim-Avancini, Centro de Medicina Nuclear, 3° andar, LIM-21, Rua Dr. Ovídio Pires de Campos, s/n, Postal code 05403-010, São Paulo, SP, Brazil.
E-mail: chaim.tiffany@gmail.com

[Correction added on Mar 12, 2018 after issue publication: Conclusion part updated].

Accepted for publication September 28, 2017

Significant outcomes

- The diagnostic performance to discriminate adult ADHD patients from HC using MRI indices obtained in this study is clearly above chance level.
- The higher discrimination figures obtained in our male-only *post hoc* analyses may suggest that the use of a presumably more homogenous sample in regard to the neurodevelopmental origin of ADHD symptoms leads to better diagnostic performance to distinguish adult ADHD patients from HC.
- The findings reported herein represent the first neurobiological evidence supporting the individual diagnosis of ADHD specifically in adulthood, based on a sample of stimulant-naïve patients.

Limitations

- Although we recruited the largest, single-site sample of stimulant-naïve adults for combined T1-weighted and DTI scanning to date, the size of our groups may have been insufficient to minimize type-II errors as well as to prevent model overfitting.
- We used a 1.5-Tesla scanner, while use of 3-Tesla scanners is supposed to afford greater contrast for brain imaging measurements.

Introduction

Attention-deficit/hyperactivity disorder (ADHD) is a highly prevalent and potentially disabling neurodevelopmental disorder in children and adolescents (1). Although relatively common in adults, the validity of the diagnosis of ADHD in adulthood has often been the subject of controversy (2, 3), and concerns have been raised that ADHD may be overdiagnosed and overtreated in adults (3, 4). Operational diagnostic criteria for childhood-onset ADHD are still in the process of full validation for adult populations (5, 6). Also, recent longitudinal investigations have suggested that many adults presenting prominent ADHD symptoms lack a history of ADHD in childhood (6–8), challenging the view that the diagnosis of ADHD in adulthood invariably represents the continuity of a childhood-onset neurodevelopmental disorder (6, 9).

Several structural magnetic resonance imaging (MRI) studies using region-of-interest (ROI) measurements or voxel-based morphometry (VBM) reported mean brain volume abnormalities in groups of children and adolescents with ADHD relative to demographically matched healthy controls (HC), often implicating prefrontal-striatal-cerebellar circuits (10, 11). There have also been MRI studies comparing groups of ADHD children against HC using diffusion tensor imaging (DTI), allowing measurements of white matter (WM) fiber myelination and organization; these have variably reported between-group mean differences in anisotropy and diffusivity within large WM tracts interconnecting brain regions thought to be critical to ADHD, such as the longitudinal fasciculi, corona radiata, internal capsule, and cingulum (12). Such MRI findings have been interpreted as reflecting a delay in brain maturation processes underlying ADHD symptoms in children and adolescents (13). Preliminary MRI studies of modestly sized adult ADHD samples have suggested the presence of mean gray matter (GM) and WM volume abnormalities, reported as more subtle than those found in children with ADHD (10, 14, 15). Yet, some of these brain abnormalities, for instance in regard to striatal volumes, appear to lose its significance in the transition to adulthood (10). DTI studies have also shown anisotropy and diffusivity alterations in WM tracts in symptomatic ADHD adults compared to HC (16, 17); however, microstructural WM abnormalities seem to be more strongly associated with ADHD symptoms in childhood than in adulthood (15).

Recently, high-dimensional pattern classification techniques using machine learning (ML) approaches have allowed the detection of spatially complex patterns of brain abnormalities in individuals suffering from psychiatric disorders, in studies employing MRI or other neuroimaging modalities (18, 19). ML algorithms allow the assessment of all brain compartments simultaneously using structural (morphometric) MRI data, as well as the generation of classifiers combining information from different neuroimaging modalities in the same subject; because of such multivariate nature of ML methods, improved sensitivity is afforded to uncover subtle abnormalities that concurrently affect more than one brain compartment in individual cases (20). ML methods have been used to identify neurobiologically distinct clinical sub-phenotypes of major psychiatric disorders (21) or to identify MRI-based brain abnormalities specific to a given diagnostic category as compared to others (22–24). Because pattern classification approaches are able to separate patients from HC at an individual basis, results of ML-based MRI studies hold potential to endorse the validity of newly recognized psychiatric categories by providing external neurobiological measures significantly above chance level to discriminate patients with a given combination of symptoms from HC (25). For such purpose, ML methods may be more fruitful compared to the conventional neuroimaging study designs above, as these rely largely on the significance of probability values extracted from univariate group-mean comparisons of brain measurements between patients and HC (19). Moreover, by identifying neuroanatomical signatures related to specific domains of psychiatric

symptoms, ML methods hold promise to provide additional objective information that could influence treatment decisions in individual cases (24). Among ML algorithms, support vector machine (SVM) has been one of the most often used classifiers in neuroscience research in the last decade (26). SVM can map features in high-dimensional space using either linear or non-linear functions (27). Non-linear SVM extends the linear SVM approach by mapping no-linearly separable data into a new higher-dimensional feature space in which a linear threshold can be used (28).

There have been several studies applying SVM and other ML methods to both structural and functional MRI data acquired from children and adolescents with ADHD, some of which use large patient samples (19, 26, 29). These studies have shown that neuroanatomical measurements may significantly discriminate ADHD patients from HC, with diagnostic accuracy indices of up to 90% (29). The use of ML in adults with ADHD seems to be more challenging, because brain abnormalities in this population are reported as more subtle than in children with ADHD. Therefore, it is relevant to investigate whether ADHD-related neuroanatomical changes in adult populations retain significant in ML-based classification analyses. However, the literature with ML methods is scarce and has been restricted to samples of up to 23 adults with ADHD. Such limited power, added to the high inter-individual clinical variability of ADHD in adults (30, 31) may have, to date, prevented the identification of a neuroanatomical signature with sufficient sensitivity and specificity to discriminate adult ADHD patients from controls on an individual patient basis. Moreover, no study to date has applied ML methods to MRI data acquired in adults who had not been previously exposed to pharmacological treatment for ADHD. Previous MRI studies have shown that treatment with stimulants may ameliorate ADHD-related structural brain abnormalities in the basal ganglia and limbic/paralimbic regions such as the anterior cingulate cortex (32–34). Therefore, the investigation of adult samples never treated with stimulants may provide information of critical relevance on brain abnormalities associated with ADHD without the confounding influence of medication effects. Given the controversies that often surround the clinical diagnosis, neurodevelopmental origin, and treatment of ADHD in adults (3, 4), the ML approach may be particularly informative to ascertain the frequency with which adults clinically diagnosed with childhood-onset ADHD may be correctly classified using MRI data acquired before treatment for ADHD.

Aims of the study

Using a single-site sample of adult attention-deficit/hyperactivity disorder patients, we report results of what, to our knowledge, is the first large multimodal (morphometric and diffusion tensor imaging) magnetic resonance imaging study applying machine learning methods to directly investigate the degree to which such neuroimaging measures discriminate individuals fulfilling diagnostic criteria for childhood-onset attention-deficit/hyperactivity disorder in adulthood, stimulant-naïve (and predominantly naïve to the use of any psychotropics), from age- and gender-matched healthy controls. We predicted that, using a non-linear support vector machine, neuroimaging measures would discriminate attention-deficit/hyperactivity disorder patients from healthy controls on an individual basis with a classification performance well above chance level (and a P value for accuracy >0.05). We also predicted that best discrimination would be obtained with classifiers combining multimodal magnetic resonance imaging information from structural and diffusion tensor imaging datasets.

Material and methods

Subjects

Adults aged between 18 and 50 years presenting symptoms compatible with the diagnosis of ADHD and stimulant-naïve were recruited from two sources: the screening service of the outpatient ADHD clinic (PRODATH) of the Institute of Psychiatry, University of São Paulo, Brazil; and a pool of individuals who responded to advertisements in the Internet and other media channels (local radios and newspapers). The HC group included volunteers recruited through advertisement in the local community.

Potentially eligible subjects underwent a detailed psychiatric interview using: the Structured Clinical Interview (SCID) for Diagnostic and Statistical Manual for Mental Disorders, 4th edition (DSM-IV) (35); and ADHD-related items from an adapted version of the Schedule for Affective Disorders and Schizophrenia for School Aged Children (K-SADS-E) (36). To ascertain the presence of a current, full diagnosis of ADHD, the DSM-IV diagnostic criteria for ADHD (35) were used, as follows: (i) presence of at least six inattention items from the DSM-IV, at least six hyperactivity/impulsivity items, or both during the past six months; (ii) chronic course of ADHD symptomatology from childhood into adulthood; and (iii)

impairment in various functionality domains because of ADHD symptoms (at work, home, and in relationships with family and friends). At the time of the evaluation of our sample, the DSM-5 criteria for diagnosing ADHD were under revision, with a proposal to increase the age of onset criterion from 7 to 12 years. This was based on findings showing a high similarity between ADHD cases with early (7 years or less) onset and ADHD cases with a later age of disease onset (5, 37–39). The proposal of changing the ADHD age of onset criterion is also based on the fact that the use of an early age of onset cutoff may lead to high false negative diagnostic rates because of biased retrospective recall (40). Such arguments based our decision to include all participants that reported onset of ADHD symptoms up to 12 years of age. Presence of other Axis I psychiatric diagnoses was established through the SCID. For the assessment of symptom severity, we used the Adult ADHD Self-Report Scale (ASRS-18) (41), the Global Assessment of Functioning (GAF) from DSM-IV (35), and the Clinical Global Impression (CGI) scale (42).

All subjects in the HC group also underwent detailed psychiatric interview using the SCID and K-SADS-E screening. Data regarding ASRS-18 scores were also available for most individuals in the HC group.

ADHD patients were excluded if reporting lifetime or current history of any other major psychiatric disorder, with the exception of mild depressive episodes, anxiety disorders, and disruptive behavior disorders. Ten ADHD subjects had been previously treated with antidepressants (up to 3 months), and they had been drug-free for at least 48 months. For details on ADHD and HC evaluation and exclusion criteria, see the Appendix S1 in the online edition of this article.

A total of 67 stimulant-naïve subjects (52 males) and 66 HC (44 males) were enrolled. As our primary aim was to investigate the value of neuroimaging predictors only (free from any additional discriminative influence of demographic variables (43), we initially restricted the analyses to ADHD (n = 58) and HC (n = 58) subjects that were individually matched for gender and second for age (within 3 years), and group-matched for years of education and socioeconomic status. Subsequently, we carried out classification analyses using a male-only subsample: ADHD (n = 52) and HC (n = 44) subjects, matched for age (within 3 years), years of education, and socioeconomic status. Taken together these two sets of analyses, all ADHD and HC individuals from the overall sample were used. Given the limited sample size of the female ADHD and HC subgroups, we refrained from carrying out female-only classification analyses. In a subset of 34 ADHD patients and 42 HC, data were available regarding smoking habits and there were no significant between-group differences (see the Appendix S1 for details).

This study was approved by the local and national ethics committees. After complete description of the study to the subjects, written informed consent was obtained.

Image acquisition

All subjects underwent MRI scanning in a 1.5T Siemens Espree system (Siemens, Erlangen, Germany). Details regarding acquisition parameters of T1-weighted and DTI data and inspection of datasets are given in the Appendix S1.

Processing and statistical analysis of neuroimaging data

T1-weighted images were preprocessed by correcting for signal inhomogeneities and removing extracerebral tissue, and automatically segmented into 259 expert-defined anatomical ROIs using a state-of-the-art multi-atlas label fusion method (44). Details of image processing steps are described in the Appendix S1.

For each ROI, together with the volume (primary T1 features), a set of additional metrics was calculated for quantifying various morphometric, intensity, and texture features (extended T1 features).

DTI sets were reconstructed from the diffusion-weighted MRI data using multivariate linear fitting (45). Voxelwise maps of fractional anisotropy (FA), trace (TR), radial, and axial diffusivity were computed for each subject (46) and spatially normalized against a standard DTI template, resulting in 176 anatomical ROIs (for details, see the Appendix S1). Following spatial normalization, the non-zero count, mean, and standard deviation of each DTI map within each ROI were calculated (primary DTI features). A set of additional metrics was also calculated for quantifying various intensity and texture features of the segmented ROIs (extended DTI features).

Models using extended T1 and DTI feature sets included all features for each ROI (primary T1 features + additional features) (for details, see the Appendix S1).

The main motivation for the experiments using the richer extended features was to investigate whether we could capture possible structural and WM tracts changes (for instance regarding tissue contrast) beyond the atrophy and DTI abnormal

values reflected by the conventional volumes and anisotropy/diffusivity indices of the ROI. Also, our choice to directly input all features to an SVM classifier was based on the fact that SVM is a very good tool to handle high-dimensional data, specifically by finding the maximum-margin separating hyperplane (27).

Primary and extended T1 and DTI features were used as inputs to non-linear SVM analyses with a Gaussian Radial Basis Function (GRBF) kernel (for details, see the Appendix S1). Considering a situation with very high dimensional input, there is a high likelihood that the data are linearly separable in the original space and therefore no need for a non-linear kernel (47). However, for smaller-dimensional data (for instance when using ROIs, that summarize each subject's brain with a relatively low-dimensional vector), exploring non-linear combinations of the input features may help to increase classification accuracy (48).

To investigate the discriminative power of each individual feature type, we performed experiments using different combinations of imaging feature sets independently. All experiments were performed using 10-fold cross-validation and repeated 100 times with random shuffling of the samples to obtain a robust order-invariant estimation of performance (see Appendix S1 for details). Permutation tests were performed to assign a significance (P) value to each classification score, by applying the classification 10000 times with the same input features but with randomly permuted class labels. Classification scores were evaluated by computing receiver operating characteristic (ROC) curves and by calculating the area under the curve (AUC) (for further information, see the Appendix S1). Diagnostic performance indices were calculated using 2×2 contingency tables, including diagnostic accuracy (DA; overall classification rate), sensitivity, specificity, positive predictive value, and negative predictive value.

Discrimination maps

The non-linear GRBF kernel method used in the above analyses does not allow estimation of which features/brain regions contribute most to the SVM decision. Therefore, we run additional multivariate analyses using a linear kernel SVM classifier and with multimodal voxelwise image data as input (see Appendix S1). Weight values were calculated for the SVM model trained with input maps, and the statistical significance was estimated for each weight value voxel using a permutation test-based inference method (49). Discrimination maps showing significant brain regions ($P < 0.05$, uncorrected) that contributed most to the classifier decision were generated for GM and WM volumes, FA and TR; the decision to report regional results for these four input modalities was taken based on the observation that, when applied individually to the non-linear SVM classifier, other feature sets obtained relatively lower accuracy in

Table 1. Sociodemographic, diagnostic, and clinical characteristics of ADHD and HC groups

	Overall ADHD group ($n = 67$)	Mixed-gender ADHD subgroup ($n = 58$)	HC subgroup with males/females ($n = 58$)	P value	Male-only ADHD subgroup ($n = 52$)	Male HC subgroup ($n = 44$)	P value
Mean age in years (SD)	27 (6.0)	26.9 (5.4)	26.7 (5.7)	0.99[b]	27 (5.1)	27 (5.5)	0.99[b]
Gender (male)	52	44	44	1[a]	–	–	–
Handedness (right)	63	55	56	0.65[a]	49	43	0.4[a]
Mean years of education (SD)	13.5 (2.6)	13.6 (2.6)	13.6 (3.2)	0.97[b]	13.6 (2.6)	13.7 (3.5)	0.8[b]
Socioeconomic status (A1 + A2/B1 + B2/C1 + C2/D/E	7/33/23/4/0	6/30/18/4/0	7/31/20/0/0	0.24[a]	7/24/19/2/0	7/23/14/0/0	0.55[a]
Disease duration*	Since childhood	Since childhood	–		Since childhood	–	
Diagnostic subtype†	36 Inattentive	30 Inattentive	–		25 Inattentive	–	
	31 Combined	28 Combined	–		27 Combined	–	
Mean ASRS							
Part A (SD)*	29.5 (3.2)	29.5 (3.2)	10.3 (4.5)‡		29.6 (3.4)	10.5 (4.9)‡	
Part B (SD)*	23.3 (7.1)	23.4 (7.1)	7.7 (4.1)‡		24.1 (6.7)	7.6 (4.2)‡	
Mean CGI (SD)*	4.5 (0.5)	4.3 (0.5)	–		4.3 (0.5)	–	
Mean GAF (SD)*	60.1 (6.3)	59.9 (5.8)	–		60.7 (6.7)	–	

ADHD, attention-deficit hyperactivity disorder; HC, healthy control; ASRS, Adult ADHD Self-Report Scale; GCI, Clinical Global Impression; GAF, Global Assessment of Functioning; SD, standard deviation; L, left; R, right.

Descriptive analyses between groups were performed by means of Chi-squared tests for categorical data ([a]) and t-tests for continuous data ([b]) t- tests.

*All patients reported the beginning of symptoms before 12 years of age, but most of them could not precise exactly the age of disease onset.

†At the time of enrollment in the study.

‡ASRS scores from 46 individuals used in the mixed-gender analysis and from 35 individuals included in the male-only analysis.

discriminating between the ADHD and HC groups.

Results

Demographic and clinical data

Demographic and clinical data for ADHD patients and HC in both the mixed-gender and male-only subgroups are summarized in Table 1. Comparisons between male and female ADHD patients in the mixed-gender subgroup revealed no significant differences in regard to scores on ASRS-18 Part A ($t = 0.24$, $P = 0.0807$), Part B ($t = 1.51$, $P = 0.135$), GAF ($t = 1.31$, $P = 0.196$), or CGI ($t = 0.58$, $P = 0.562$) scales.

Comorbid psychiatric diagnoses were present in 12 ADHD subjects and 1 HC, and these are listed in the Appendix S1. In the HC group, ASRS scores were available for 46 individuals used in the mixed-gender analysis (mean ASRS: Part A = 10.3, SD = 4.5; Part B = 7.7, SD = 4.1) and for 35 individuals included in the male-only analysis (mean ASRS: Part A = 10.5, SD = 4.9; Part B = 7.6, SD = 4.2). Such ASRS-18 scores indicated the absence of any meaningful hyperactivity/inattentive features. For those HC individuals whose ASRS-18 score was missing ($n = 12$), the detailed psychiatric interview discarded the presence of inattention and/or hyperactivity symptoms in any subjects.

Diagnostic performance of SVM classifiers using the GRBF kernel

In the mixed-gender analyses (ADHD, $n = 58$ vs HC, $n = 58$), best classification performance was obtained by combining morphometric and DTI features (Table 2). Specifically, the classification using primary T1 and DTI features resulted in AUC and DA of 0.71% and 65.4% ($P = 0.005$) respectively. A higher AUC here indicates a better relationship between specificity and sensitivity and therefore a more optimal/robust classification model. In the comparison of individual MR imaging modalities, DTI features in isolation achieved better AUC and DA (Table 2). Figure 1 shows ROC curves for the best AUC achieved by the combination of T1 and DTI features as well as when using only DTI or T1 features.

In the classification experiments using the male-only subsamples (Table 2 and Fig. 2), best classification performance was also obtained by the combination of primary T1 and DTI features (AUC = 0.74; DA = 74%; $P = 0.0001$). DTI features used alone achieved higher AUC and DA compared to T1 features alone, but the accuracy was lower than the one obtained using the combination of T1 and DTI features (Table 2). The classification accuracy for the male-only sample was consistently higher than the one obtained for the mixed-gender sample.

Considering that the T1 features used in isolation did not show any predictive value in our classification analyses but added a slight contribution in the classification performance when used in combination with DTI features, we decided to test the significance of the difference between the classifications using DTI alone and DTI and T1 features together using an independent t-test. The addition of the T1 features created a significant increase in the accuracy ($P = 0.01$ for the mixed-gender subsamples and $P = 0$ 5.4397E-10 for the male-only subsamples).

Table 2. Diagnostic performance of the GRBF kernel SVM classifier in the individual discrimination between mixed-gender ADHD ($n = 58$) and HC ($n = 58$) subgroups and between male-only ADHD ($n = 52$) and HC ($n = 44$) subgroups, using only primary features

	Features used	AUC, mean (SD)	Accuracy (%), mean (SD)	Sensitivity*(%), mean (SD)	Specificity† (%) mean (SD)	Positive predictive value (%), mean (SD)	Negative predictive value (%), mean (SD)	False positive rate (%), mean (SD)	False negative rate (%), mean (SD)	False discovery rate (%), mean (SD)	*P* value‡
Mixed-gender subgroups	Primary T1	0.534 (0.04)	52.6 (0.04)	44.8 (0.07)	60.4 (0.06)	53.0 (0.05)	52.3 (0.04)	39.6 (0.06)	55.2 (0.07)	48.4 (0.05)	0.29
	Primary DTI	0.685 (0.01)	65.4 (0.02)	54.9 (0.02)	75.9 (0.02)	69.9 (0.03)	62.7 (0.01)	24.1 (0.03)	45.1 (0.02)	30.3 (0.02)	0.005
	Primary T1 + Primary DTI	0.714 (0.01)	65.4 (0.02)	56.7 (0.02)	74.0 (0.02)	68.6 (0.02)	63.1 (0.02)	26.0 (0.02)	43.3 (0.02)	31.8 (0.02)	0.01
Male-only subgroups	Primary T1	0.608 (0.03)	57.9 (0.02)	35.0 (0.05)	77.3 (0.03)	56.5 (0.04)	58.4 (0.02)	22.7 (0.03)	65.0 (0.05)	43.5 (0.04)	0.11
	Primary DTI	0.710 (0.01)	72.4 (0.02)	57.2 (0.01)	85.2 (0.03)	76.7 (0.04)	70.2 (0.01)	14.8 (0.03)	42.8 (0.01)	23.3 (0.04)	0.0001
	Primary T1 + Primary DTI	0.742 (0.01)	73.8 (0.02)	58.4 (0.02)	86.8 (0.03)	79.1 (0.04)	71.1 (0.01)	13.2 (0.03)	41.6 (0.02)	20.9 (0.04)	0.0001

ADHD, attention-deficit/hyperactivity disorder; HC, healthy control; SD, standard deviation; primary T1, regions of interest (ROIs) for gray matter and white matter volumes; primary DTI, fractional anisotropy, trace, radial diffusivity, and axial diffusivity ROIs; AUC, area under the curve.

*Displays the true positive rate in the ADHD male/female subgroup.

†Displays the true negative rate in the ADHD male/female subgroup.

‡Statistical significance for accuracy.

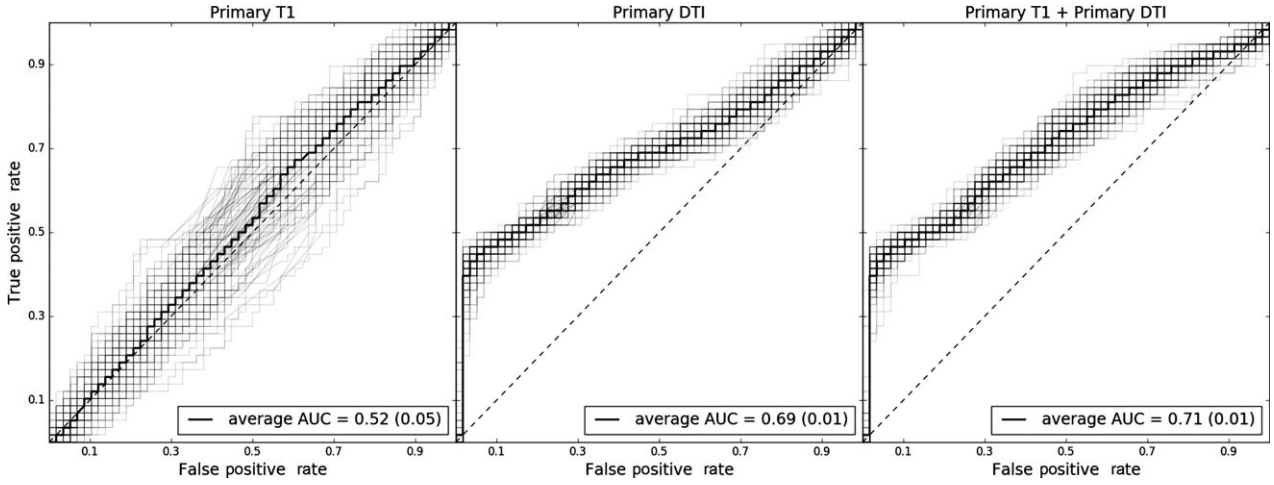

Fig. 1. ROC curves for the best AUC obtained from the GRBF kernel SVM analyses using brain volumetric and DTI inputs separately and combined to distinguish mixed-gender ADHD (n = 58) from HC (n = 58) subjects. The gray curves indicate each individual trial, and the bold black curve indicates the mean ROC. ROC, receiver operating characteristic; primary T1, regions of interest (ROIs) for gray matter and white matter volumes; primary DTI, fractional anisotropy, trace, radial diffusivity, and axial diffusivity ROIs; AUC, area under the curve.

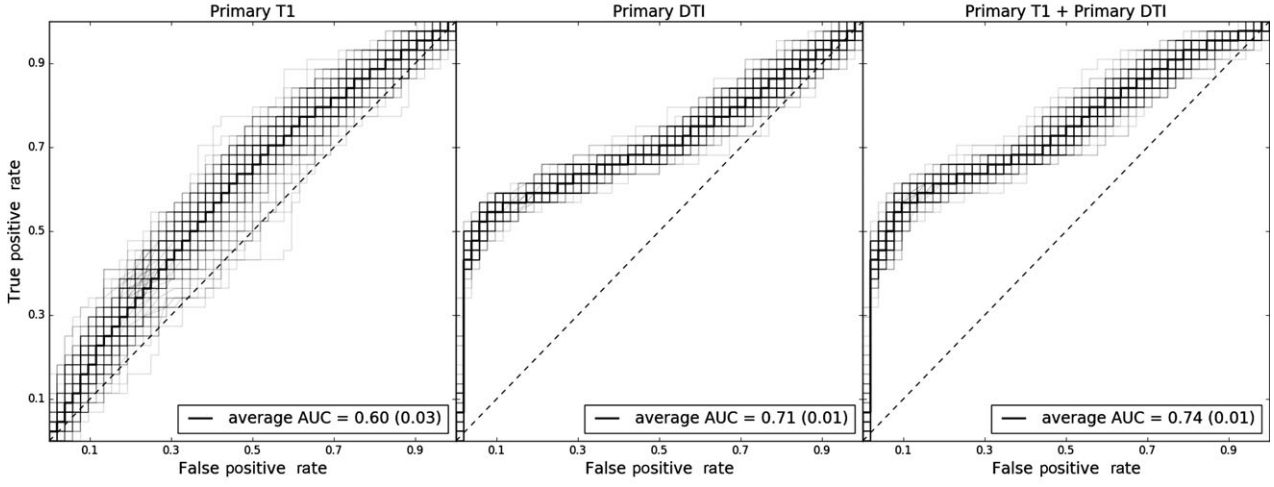

Fig. 2. ROC curves for the best AUC obtained from the GRBF kernel SVM analyses using brain volumetric and DTI inputs separately and combined to distinguish male-only ADHD (n = 52) from HC (n = 44) subjects. The gray curves indicate each individual trial, and the bold black curve indicates the mean ROC. Primary T1, regions of interest (ROIs) for gray matter and white matter volumes; primary DTI, fractional anisotropy, trace, radial diffusivity, and axial diffusivity ROIs; AUC, area under the curve.

In both sets of experiments, higher specificity than sensitivity figures were obtained (see Table 2), indicating a higher probability of correctly identifying individuals who are not ADHD patients than an ability to detect ADHD patients (50).

Classification results for the mixed-gender and male-only samples using the extended ROI features are shown in Table S1 (data supplement). We found that the use of extended morphometric and DTI features did not improve the classification accuracy in general, in comparison with results obtained using only primary features.

Discrimination maps using linear SVM

Performance figures obtained using the linear classification were all above chance level (see Table S2 in the data supplement). Representative sections showing brain regions that were found to be discriminative between mixed-gender ADHD patients and HC are shown in Fig. 3, for each of the four selected input image modalities (GM, WM, FA, and TR).

The neuroanatomical pattern using volumetric measures showed high discriminative weights ($P < 0.05$, uncorrected) in widespread GM and

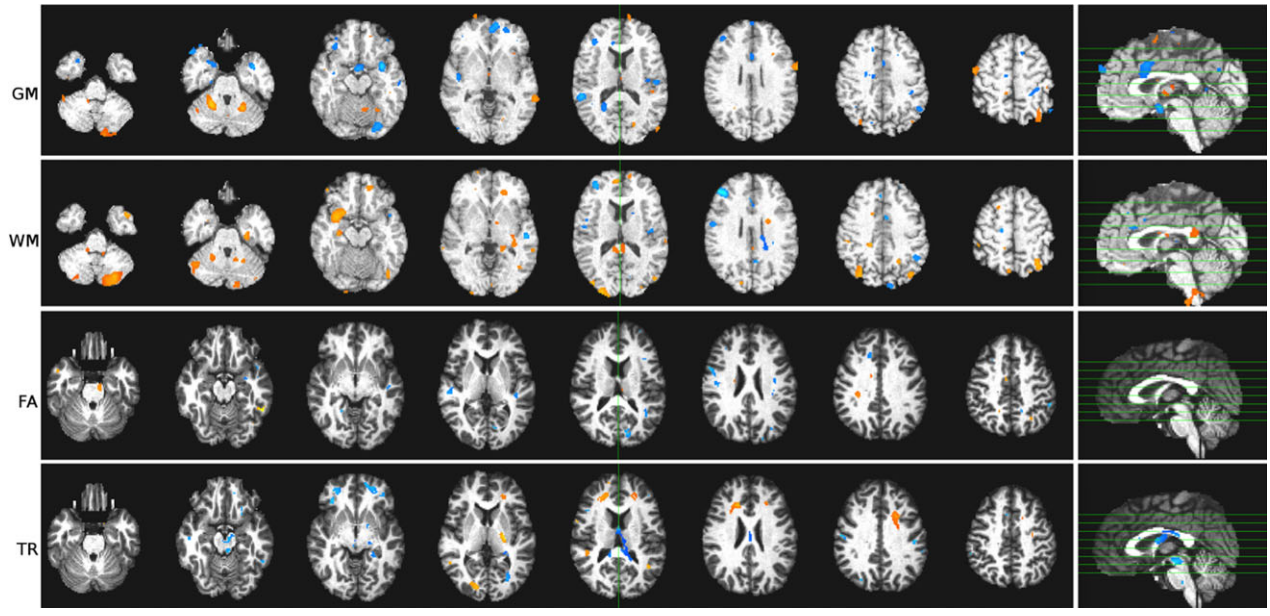

Fig. 3. Representative sections of the spatial maps showing the pattern of morphometric and DTI regions used by the linear SVM classifier to discriminate between mixed-gender ADHD (n = 58) and HC (n = 58) subgroups. Discrimination maps were identified by selecting the weight vector scores at $P < 0.05$ (uncorrected for multiple comparisons). Warm colors (positive weights) indicate higher parameter values for ADHD than HC subjects. Cool colors (negative weights) indicate higher parameter values for HC than ADHD subjects. GM, gray matter volume; WM, white matter volume; FA, fractional anisotropy, TR, trace.

WM regions across the frontal, temporal, parietal, and occipital lobes, as well as the cingulate gyrus, insula, thalamus, and cerebellum (see Figures S1 and S2 and Table S3 in the data supplement for details). The DTI analyses showed high weights ($P < 0.05$, uncorrected) in several bilateral WM regions both for FA and TR indices, involving the corticospinal tracts, inferior and superior longitudinal fasciculi, inferior fronto-occipital fasciculus, uncinate fasciculus, corpus callosum, fornix, cingulum, thalamic radiations, superior corona radiata, middle cerebellar peduncle, and brain stem (see Fig. 3 and also Figures S3 and S4 and Table S4 in the data supplement). The male-only subgroup analyses resulted in similar results (see Figures S5–S8 in the data supplement).

Discussion

To the best of our knowledge, this is the first MRI study applying ML methods to compare a relatively large group of stimulant-naïve ADHD adults (and predominantly naïve to the use of any psychotropics) to HC, all recruited from the same community and scanned at a single MRI site. We confirmed our prediction that the diagnostic performance to discriminate adult ADHD patients from HC using MRI indices would be well above chance level. The possibility of assessing stimulant-naïve ADHD patients on an individual basis gives us the opportunity of capturing information about the pathophysiology underlying the symptoms of ADHD without the bias of treatment-induced brain alterations. Because all previous ML-based MRI studies of adults never treated for ADHD symptoms were carried out using child and adolescent samples (51, 52), the findings reported herein represent the first neurobiological evidence supporting the individual diagnosis of stimulant-naïve ADHD patients specifically in adulthood. The diagnostic performance achieved in our study is similar to that reported in recent, large-scale ML-based MRI studies investigating potentially severe psychiatric disorders in adults such as schizophrenia (24, 53) and better than figures reported in studies of other major mental conditions such as bipolar disorder (24, 54).

As we aimed to obtain diagnostic performance indices that could be related specifically to the inattention-hyperactivity dimensions that characterize the ADHD diagnosis, we deliberately excluded individuals presenting major psychiatric comorbidities relatively common in adult ADHD patients, such as bipolar disorder (55). This strategy aimed to minimize the variability that would be potentially added to imaging measurements by such comorbidity. Other major psychiatric disorders (i.e., anxiety disorders) were detected in <15% of ADHD patients, and it is therefore highly unlikely that the presence of such additional diagnoses

contributed significantly to the ADHD-related neuroanatomical signature reported herein.

One should note that when morphometric and DTI measures were used alone for classification, best performance was obtained using DTI features. This agrees with a view that abnormalities in WM tract myelination and organization play a prominent role in ADHD pathophysiology (16, 17). Morphometric features (involving both the GM and WM compartments) added a significant contribution in the classification performance when used in combination with DTI features, but had a poor predictive power in isolation. This may suggest that in our non-linear SVM classification, although morphometric brain changes in isolation were not able classify the groups, they added useful information during some point of the analysis (e.g., assisting the selection algorithm to extract the most discriminative features from the poll (56) that contributed for constructing the classification model. This agrees with the results of previous morphometric and DTI studies that performed mean group comparisons between ADHD adults and HC, as these studies have reported subtle GM (57) and WM volume abnormalities (58) and abnormal DTI indices (12) in ADHD.

In our study, the use of extended features did not lead to improved models, as compared to the primary feature models. A potentially large number of features extracted from images (bringing informative and/or non-informative features for the classifier) and a modest number of samples available for training can increase the susceptibility of the classification model to overfitting (59–61). Although previous studies reported that the use of some additional feature measures (such as intensity and shape) can improve the classification performance in psychiatric disorders such as schizophrenia and Alzheimer's disease (62, 63), other investigations have shown that combining multiple feature measurements (such as folding and curvature indices in ADHD) does not afford high predictive power (56, 64). It is possible that the combination of all extended features in the classification model in the present study prevented us from finding a true contribution of one or a few of those additional feature measures, and this should be investigated in future studies.

Although the two hypotheses of the present study were confirmed, the maximal sensitivity and specificity figures obtained are typical of diagnostic tests of fair accuracy (65). In studies of psychiatric disorders in general, the performance of classifiers may vary because of etiological and phenotypic heterogeneity, which is likely to be accompanied by different biological substrates (25, 30). The fair diagnostic performance reported in our study is possibly influenced by three factors: the difficulty in clearly characterizing core ADHD symptoms as present and clinically meaningful in some adult cases (66); the overlap of ADHD symptoms with manifestations that are typical of other psychiatric disorders (67); and the inherent phenotypic heterogeneity of the ADHD diagnosis in regard to its clinical subtypes (combined inattentive/hyperactive or predominantly inattentive) (68). Regarding the latter aspect, previous ML findings on MRI data from representative children and adolescent ADHD samples have shown relatively better diagnostic accuracy when more homogeneous ADHD subgroups (in terms of clinical subtypes) are evaluated (29, 69). However, the purpose of the present study was to search for a common neuroanatomical signature that would discriminate a reasonably large adult ADHD sample (across the clinical subtypes of the disorder) from CS. Therefore, one may conclude that diagnostic figures of around 70% of DA and 0.70 of AUC (as those obtained herein) have good face validity in terms of what, in fact, is the clinical reality of the ADHD diagnosis in adults. A higher AUC indicates a better relationship between specificity and sensitivity and, therefore, a more optimal/robust classification model. The observation that our classifiers offered high specificity but limited sensitivity supports a view that some adults diagnosed as ADHD sufferers may actually present normal brain anatomy and could potentially be candidates for non-pharmacological treatment or watchful waiting.

It is interesting to note that the accuracy figures reported in our study are more modest than those described in some previous brain morphometry studies of children and adolescents with ADHD (19, 26). This gives support to a view that neuroimaging biomarkers may be less discriminating to distinguish ADHD from controls in adult life as compared to childhood. This hypothesis requires further confirmatory ML studies with larger samples and use of multimodal neuroimaging data in both age groups.

The discriminative maps obtained from linear SVM analyses using volumetric measurements were used with the exploratory aim of assessing the pattern of regional brain distribution of discriminative features between groups. This analysis indicated that several cortical, subcortical, and cerebellar brain regions previously implicated in ADHD pathophysiology (11, 13, 57) contributed to classification. The neuroanatomical feature selection of WM tracts was also consistent with findings of recent DTI studies comparing groups of ADHD subjects vs. HC (11, 12, 16, 17). However, these spatial distribution patterns should be

interpreted cautiously, given that the significance maps derived from SVM are uncorrected for multiple comparisons and somewhat spotty. For a VBM type of mean group comparison, such statistical results might have been interpreted as of weak significance. Nevertheless, it is important to stress that SVM analyses are different from conventional group comparisons in two respects. First, SVM is a single test, as opposed to many tests applied in mass-univariate analyses; second, an SVM classifier has a strong regularization term to select only the smallest possible set of features (brain regions, herein) that achieve best classification. Therefore, the statistical maps (Fig. 3 and Figures S1–S8) should be seen as solely reflecting samples of regions used to derive classification scores, rather than the disease effects in their entirety.

Childhood-onset ADHD symptoms are thought to be the consequence of neurodevelopmental abnormalities (11, 70), and it is known that there is a marked male preponderance in the overall incidence of neurodevelopmental disorders (71). The discrimination figures obtained in our male-only *post hoc* analyses were somehow higher than the indices found in the overall mixed-gender analyses. This might suggest that the use of a presumably more homogenous sample in regard to the neurodevelopmental origin of ADHD symptoms leads to better diagnostic performance to distinguish adult ADHD patients from HC (reflecting a greater degree of deviation from normality for the brains of male ADHD patients). However, this possibility has to be raised with great caution; we were not able to also conduct female-only analyses because of limited sample size, and we cannot therefore rule out the alternative explanation that the greater AUC values in the male-only analyses simply reflected the use of a gender-homogeneous sample. Nevertheless, it is interesting to note that one recent ML-based structural MRI study of prototypical neurodevelopmental autism spectrum disorders showed a similar degree of improvement on discrimination performance in male-only SVM analyses, but not in analyses restricted to a female subgroup of the same size (72). Thus better, classification results in male-only SVM analyses carried out with disorders such as autism or childhood-onset ADHD may not simply be because of the use of homogeneous groups in regard to gender. Instead, such increased male-only discrimination ability might reflect a greater degree of brain structural deviation from normality, as expected in neurodevelopmental disorders.

Neuroimaging literature on psychiatric disorders has recently undergone fierce criticism, particularly given difficulties to avoid the influence of confounders that vary systematically between patient and HC groups, such as use of psychoactive medication or substance abuse, metabolic variations, medical comorbidities, and smoking habits (63). Fortunately, we were able to rule out the influence of several of those variables, because we strictly excluded subjects previously treated for ADHD symptoms or who had recently received any psychiatric treatment, as well as individuals with previous history of drug abuse or general medical conditions. Moreover, data collected in representative subsamples of our ADHD and HC groups suggested no significant differences in smoking habits. Also, our analyses lined-up the same number of subjects in ADHD and HC groups individually matched for age and gender and group-matched for socioeconomic status and education. This assures us that the discrimination between groups would have been predominantly driven by the ADHD phenotype rather than by such demographic variables (43).

In ML studies, accuracy indices that are significantly above chance level do not imply that findings can be applicable in clinical practice. Our pattern recognition algorithms was trained and tested on groups of a relatively modest size and, therefore, accuracies that are derived from those samples are not directly representative for predictions in clinical populations (19, 73). The performance indices of fair accuracy obtained in the present study are consistent with the notion that there are important limitations in the application of ML techniques for predicting diagnosis in clinical neuroimaging research (73, 74). Despite several promising results (19, 26), there are many challenges that still need to be addressed before these techniques can be seen as promptly applicable to make psychiatric diagnostic predictions. These include the need for more methodological advances in combination with comprehensive validation studies using larger, multimodal, and prospectively acquired datasets to enable the acquisition of more accurate patter recognition models (19, 75). Such studies have not yet been carried out (19, 75). Thus, to validate the use of ML-based neuroimaging findings in clinical practice, results such as those reported in the present study should be extended in larger, population-based investigations evaluating adults presenting ADHD spectrum symptoms across the entire range of severity and comorbidities. Despite such future challenges, ML techniques might be a useful adjunctive tool in the short and medium term that to assist complex clinical decisions in specific diagnostic settings. Specifically in regard to ADHD in adults, such latter applications may be of interest, for instance, to disentangle

ADHD from comorbidities such as bipolar disorder, once there are several points of pathophysiological overlap as well as admixture of clinical manifestations between these two disorders (76, 77). Also, besides the efforts to bring ML techniques to the clinical practice, one should stress that pattern recognition techniques are an important tool for discovering brain mechanisms involved in ADHD because the multivariate approaches have potentially high sensitivity for detecting subtle and distributed brain alterations.

A number of limitations of the present study should be highlighted. First, there are limitations in regard to the use of a 1.5-Tesla scanner and the DTI acquisition protocol employed, which are addressed in the data supplement. Second, although we managed to recruit the largest, single-site sample of stimulant-naïve ADHD adults for combined T1-weighted and DTI scanning to date, the size of our groups may have been still insufficient to minimize type-II errors. Although SVM is a ML method that is less sensitive to sample size variations, a limited number of data samples can cause model overfitting, resulting in poor generalization of the method in independent datasets (78). This may at least partially explain findings of different predictive accuracies that have been reported across separate samples of the same disorder assessed using exactly the same diagnostic criteria and symptom rating scales, as well as similar MRI data acquisition protocols (79). Therefore, future MRI studies with even larger samples of stimulant-naïve ADHD adults may be needed to confirm the findings reported herein. However, because it is difficult to recruit representative populations of stimulant-naïve ADHD adults from a single-site, larger ML-based studies combining data from multiple sites (obtained with the same selection criteria) may be considered as a more feasible alternative (79). Such multi-site MRI studies should allow both the testing of diagnostic performance across independent validation samples of adults never treated for ADHD symptoms (23), and the use of novel multi-task learning methods suitable for finding disease-related signatures while handling heterogeneity across different populations and MRI acquisition protocols (80, 81).

In conclusion, the present ML-based investigation using brain morphometric and DTI indices provided, for the first time, external neurobiological measurements that discriminated stimulant-naïve adults fulfilling clinical diagnostic criteria for childhood-onset ADHD from HC on an individual basis, with classification performance significantly above chance level. Although not at the levels of clinically definitive diagnostic accuracy, the neuroanatomical signature of ADHD reported herein may provide additional and objective information that could influence treatment decisions in adults with ADHD spectrum symptoms. Further ML studies are now warranted to investigate whether baseline brain MRI patterns may predict treatment response and diagnostic stability over time in stimulant-naïve ADHD adults.

Acknowledgements

The present investigation was supported by a 2010 NARSAD Independent Investigator Award (NARSAD: The Brain and Behavior Research Fund) awarded to Geraldo F. Busatto. Geraldo F. Busatto is also partially funded by CNPq-Brazil. Marcus V. Zanetti is funded by FAPESP, Brazil (no. 2013/03905-4).

Declaration of interest

All the authors declare to have no conflicts of interest, reporting no financial relationships with commercial interests pertaining to this article.

References

1. Polanczyk G, Rohde LA. Epidemiology of attention-deficit/hyperactivity disorder across the lifespan. Curr Opin Psychiatry 2007;**20**:386–392.
2. National Collaborating Centre for Mental H. National Institute for Health and Clinical Excellence: Guidance. Attention deficit hyperactivity disorder: diagnosis and management of ADHD in children, young people and adults. Leicester, UK: British Psychological Society (UK) The British Psychological Society & The Royal College of Psychiatrists, 2009.
3. Ramos-Quiroga JA, Nasillo V, Fernandez-Aranda F, Casas M. Addressing the lack of studies in attention-deficit/hyperactivity disorder in adults. Expert Rev Neurother 2014;**14**:553–567.
4. Paris J, Bhat V, Thombs B. Is adult attention-deficit hyperactivity disorder being overdiagnosed? Can J Psychiatry 2015;**60**:324–328.
5. Matte B, Rohde LA, Turner JB et al. Reliability and validity of proposed DSM-5 ADHD symptoms in a clinical sample of adults. J Neuropsychiatry Clin Neurosci 2015;**27**:228–236.
6. Moffitt TE, Houts R, Asherson P et al. Is adult ADHD a childhood-onset neurodevelopmental disorder? Evidence from a four-decade longitudinal cohort study. Am J Psychiatry 2015;**172**:967–977.
7. Caye A, Rocha TB, Anselmi L et al. Attention-deficit/hyperactivity disorder trajectories from childhood to young adulthood: evidence from a birth cohort supporting a late-onset syndrome. JAMA Psychiatry 2016;**73**:705–712.
8. Agnew-Blais JC, Polanczyk GV, Danese A, Wertz J, Moffitt TE, Arseneault L. Evaluation of the persistence, remission, and emergence of attention-deficit/hyperactivity disorder in young adulthood. JAMA Psychiatry 2016;**73**:713–720.
9. Castellanos FX. Is adult-onset ADHD a distinct entity? Am J Psychiatry 2015;**172**:929–931.
10. Frodl T, Skokauskas N. Meta-analysis of structural MRI studies in children and adults with attention deficit

hyperactivity disorder indicates treatment effects. Acta Psychiatr Scand 2012;**125**:114–126.
11. Rubia K, Alegria A, Brinson H. Imaging the ADHD brain: disorder-specificity, medication effects and clinical translation. Expert Rev Neurother 2014;**14**: 519–538.
12. Cortese S, Imperati D, Zhou J et al. White matter alterations at 33-year follow-up in adults with childhood attention-deficit/hyperactivity disorder. Biol Psychiatry 2013; **74**:591–598.
13. Shaw P, Gilliam M, Liverpool M et al. Cortical development in typically developing children with symptoms of hyperactivity and impulsivity: support for a dimensional view of attention deficit hyperactivity disorder. Am J Psychiatry 2011;**168**:143–151.
14. Onnink AM, Zwiers MP, Hoogman M et al. Brain alterations in adult ADHD: effects of gender, treatment and comorbid depression. Eur Neuropsychopharmacol 2014; **24**:397–409.
15. Gehricke JG, Kruggel F, Thampipop T et al. The brain anatomy of attention-deficit/hyperactivity disorder in young adults - a magnetic resonance imaging study. PLoS One 2017;**12**:e0175433.
16. Chaim TM, Zhang T, Zanetti MV et al. Multimodal magnetic resonance imaging study of treatment-naive adults with attention-deficit/hyperactivity disorder. PLoS One 2014;**9**:e110199.
17. Yoncheva YN, Somandepalli K, Reiss PT et al. Mode of anisotropy reveals global diffusion alterations in attention-deficit/hyperactivity disorder. J Am Acad Child Adolesc Psychiatry 2016;**55**:137–145.
18. Aydin S, Arica N, Ergul E, Tan O. Classification of obsessive compulsive disorder by EEG complexity and hemispheric dependency measurements. Int J Neural Syst 2015;**25**:1550010.
19. Wolfers T, Buitelaar JK, Beckmann C, Franke B, Marquand AF. From estimating activation locality to predicting disorder: a review of pattern recognition for neuroimaging-based psychiatric diagnostics. Neurosci Biobehav Rev 2015;**57**:328–349.
20. Lao Z, Shen D, Xue Z, Karacali B, Resnick SM, Davatzikos C. Morphological classification of brains via high-dimensional shape transformations and machine learning methods. NeuroImage 2004;**21**:46–57.
21. Wu H, Sun H, Wang C et al. Abnormalities in the structural covariance of emotion regulation networks in major depressive disorder. J Psychiatr Res 2017;**84**:237–242.
22. Costafreda SG, Fu CH, Picchioni M et al. Pattern of neural responses to verbal fluency shows diagnostic specificity for schizophrenia and bipolar disorder. BMC Psychiatry 2011;**11**:18.
23. Schnack HG, Nieuwenhuis M, van Haren NE et al. Can structural MRI aid in clinical classification? A machine learning study in two independent samples of patients with schizophrenia, bipolar disorder and healthy subjects. NeuroImage 2014;**84**:299–306.
24. Koutsouleris N, Meisenzahl EM, Borgwardt S et al. Individualized differential diagnosis of schizophrenia and mood disorders using neuroanatomical biomarkers. Brain 2015;**138**:2059–2073.
25. Farah MJ, Gillihan SJ. The puzzle of neuroimaging and psychiatric diagnosis: technology and nosology in an evolving discipline. AJOB Neurosci 2012;**3**:31–41.
26. Arbabshirani MR, Plis S, Sui J, Calhoun VD. Single subject prediction of brain disorders in neuroimaging: promises and pitfalls. NeuroImage 2017;**145**:137–165.
27. James G, Witten D, Hastie T, Tibshirani R. An introduction to statistical learning – with applications in R | Gareth James. New York: Springer, 2013.
28. Smola A, Bartelett P, Schölkopf B, Schuurmans D (Eds.). Introduction to large margin classifiers. Advances in large margin classifiers. Cambridge, MA: MIT Press, 2000:1–28.
29. Deshpande G, Wang P, Rangaprakash D, Wilamowski B. Fully connected cascade artificial neural network architecture for attention deficit hyperactivity disorder classification from functional magnetic resonance imaging data. IEEE Trans Cybern 2015;**45**:2668–2679.
30. Bruxel EM, Akutagava-Martins GC, Salatino-Oliveira A et al. ADHD pharmacogenetics across the life cycle: new findings and perspectives. Am J Med Genet B Neuropsychiatr Genet 2014;**165b**:263–282.
31. Sanefuji M, Craig M, Parlatini V et al. Double-dissociation between the mechanism leading to impulsivity and inattention in attention deficit hyperactivity disorder: a resting-state functional connectivity study. Cortex 2016;**86**:290–302.
32. Villemonteix T, de Brito SA, Kavec M et al. Grey matter volumes in treatment naive vs. chronically treated children with attention deficit/hyperactivity disorder: a combined approach. Eur Neuropsychopharmacol 2015;**25**:1118–1127.
33. Schweren LJ, de Zeeuw P, Durston S. MR imaging of the effects of methylphenidate on brain structure and function in attention-deficit/hyperactivity disorder. Eur Neuropsychopharmacol 2013;**23**:1151–1164.
34. Spencer TJ, Brown A, Seidman LJ et al. Effect of psychostimulants on brain structure and function in ADHD: a qualitative literature review of magnetic resonance imaging-based neuroimaging studies. J Clin Psychiatry 2013;**74**:902–917.
35. American Psychiatric Association. Diagnostic and statistical manual of mental disorders, 4th ed. Washington, DC: American Psychiatric Press, 1994.
36. Grevet EH, Bau CH, Salgado CA et al. [Interrater reliability for diagnosis in adults of attention deficit hyperactivity disorder and oppositional defiant disorder using K-SADS-E]. Arq Neuropsiquiatr 2005;**63**:307–310.
37. Faraone SV, Kunwar A, Adamson J, Biederman J. Personality traits among ADHD adults: implications of late-onset and subthreshold diagnoses. Psychol Med 2009;**39**:685–693.
38. Faraone SV, Biederman J, Doyle A et al. Neuropsychological studies of late onset and subthreshold diagnoses of adult attention-deficit/hyperactivity disorder. Biol Psychiatry 2006;**60**:1081–1087.
39. Faraone SV, Biederman J, Mick E. The age-dependent decline of attention deficit hyperactivity disorder: a meta-analysis of follow-up studies. Psychol Med 2006;**36**:159–165.
40. Kieling C, Kieling RR, Rohde LA et al. The age at onset of attention deficit hyperactivity disorder. Am J Psychiatry 2010;**167**:14–16.
41. Adler LA, Spencer T, Faraone SV et al. Validity of pilot Adult ADHD Self- Report Scale (ASRS) to rate adult ADHD symptoms. Ann Clin Psychiatry 2006;**18**:145–148.
42. Lima MS, Soares BG, Paoliello G et al. The Portuguese version of the Clinical Global Impression-Schizophrenia Scale: validation study. Rev Bras Psiquiatr 2007;**29**:246–249.
43. Brown MR, Sidhu GS, Greiner R et al. ADHD-200 Global Competition: diagnosing ADHD using personal characteristic data can outperform resting state fMRI measurements. Front Syst Neurosci 2012;**6**:69.

44. Doshi J, Erus G, Ou Y et al. MUSE: MUlti-atlas region segmentation utilizing ensembles of registration algorithms and parameters, and locally optimal atlas selection. NeuroImage 2016;**127**:186–195.
45. Pierpaoli C, Basser PJ. Toward a quantitative assessment of diffusion anisotropy. Magn Reson Med 1996;**36**:893–906.
46. Jones DK. Studying connections in the living human brain with diffusion MRI. Cortex 2008;**44**:936–952.
47. Hsu C, Chang C, Lin C. A practical guide to support vector classification. www.csie.ntu.edu.tw/˜cjlin/papers/guide/guide.pdf. Accessed 2017 August 29; 2016.
48. Song S, Zhan Z, Long Z, Zhang J, Yao L. Comparative study of SVM methods combined with voxel selection for object category classification on fMRI data. PLoS One 2011;**6**:e17191.
49. Gaonkar B, Davatzikos C. Analytic estimation of statistical significance maps for support vector machine based multivariate image analysis and classification. NeuroImage 2013;**78**:270–283.
50. Parikh R, Mathai A, Parikh S, Chandra Sekhar G, Thomas R. Understanding and using sensitivity, specificity and predictive values. Indian J Ophthalmol 2008;**56**:45–50.
51. Wong HK, Tiffin PA, Chappell MJ et al. Personalized medication response prediction for attention-deficit hyperactivity disorder: learning in the model space vs. learning in the data space. Front Physiol 2017;**8**:199.
52. Yoo JH, Kim D, Choi J, Jeong B. Treatment effect of methylphenidate on intrinsic functional brain network in medication-naive ADHD children: a multivariate analysis. Brain Imaging Behav 2017; https://doi.org/10.1007/s11682-017-9713-z. [Epub ahead of print].
53. Zanetti MV, Schaufelberger MS, Doshi J et al. Neuroanatomical pattern classification in a population-based sample of first-episode schizophrenia. Prog Neuropsychopharmacol Biol Psychiatry 2013;**43**:116–125.
54. Serpa MH, Ou Y, Schaufelberger MS et al. Neuroanatomical classification in a population-based sample of psychotic major depression and bipolar I disorder with 1 year of diagnostic stability. Biomed Res Int 2014;**2014**:706157.
55. Torres I, Gomez N, Colom F et al. Bipolar disorder with comorbid attention-deficit and hyperactivity disorder. Main clinical features and clues for an accurate diagnosis. Acta Psychiatr Scand 2015;**132**:389–399.
56. Qureshi MNI, Oh J, Min B, Jo HJ, Lee B. Multi-modal, multi-measure, and multi-class discrimination of ADHD with hierarchical feature extraction and extreme learning machine using structural and functional brain MRI. Front Hum Neurosci 2017;**11**:157.
57. Makris N, Liang L, Biederman J et al. Toward defining the neural substrates of ADHD: a controlled structural MRI study in medication-naive adults. J Atten Disord 2015;**19**:944–953.
58. Seidman LJ, Valera EM, Makris N et al. Dorsolateral prefrontal and anterior cingulate cortex volumetric abnormalities in adults with attention-deficit/hyperactivity disorder identified by magnetic resonance imaging. Biol Psychiatry 2006;**60**:1071–1080.
59. Wachinger C, Reuter M. Domain adaptation for Alzheimer's disease diagnostics. NeuroImage 2016;**139**:470–479.
60. Adaszewski S, Dukart J, Kherif F, Frackowiak R, Draganski B. How early can we predict Alzheimer's disease using computational anatomy? Neurobiol Aging 2013;**34**:2815–2826.
61. Mwangi B, Tian TS, Soares JC. A review of feature reduction techniques in neuroimaging. Neuroinformatics 2014;**12**:229–244.
62. Radulescu E, Ganeshan B, Shergill SS et al. Grey-matter texture abnormalities and reduced hippocampal volume are distinguishing features of schizophrenia. Psychiatry Res 2014;**223**:179–186.
63. Weinberger DR, Radulescu E. Finding the elusive psychiatric "lesion" with 21st-century neuroanatomy: a note of caution. Am J Psychiatry 2016;**173**:27–33.
64. Qureshi MN, Boreom L. Classification of ADHD subgroup with recursive feature elimination for structural brain MRI. Conf Proc IEEE Eng Med Biol Soc 2016;**2016**:5929–5932.
65. Kim YJ, Cho MJ, Park S et al. The 12-item general health questionnaire as an effective mental health screening tool for general korean adult population. Psychiatry Investig 2013;**10**:352–358.
66. Thapar A, Cooper M. Attention deficit hyperactivity disorder. Lancet 2016;**387**:1240–1250.
67. Cadman T, Findon J, Eklund H et al. Six-year follow-up study of combined type ADHD from childhood to young adulthood: predictors of functional impairment and comorbid symptoms. Eur Psychiatry 2016;**35**:47–54.
68. Willcutt EG, Nigg JT, Pennington BF et al. Validity of DSM-IV attention deficit/hyperactivity disorder symptom dimensions and subtypes. J Abnorm Psychol 2012;**121**:991–1010.
69. Sato JR, Hoexter MQ, Fujita A, Rohde LA. Evaluation of pattern recognition and feature extraction methods in ADHD prediction. Front Syst Neurosci 2012;**6**:68.
70. Shaw P, Malek M, Watson B, Greenstein D, de Rossi P, Sharp W. Trajectories of cerebral cortical development in childhood and adolescence and adult attention-deficit/hyperactivity disorder. Biol Psychiatry 2013;**74**:599–606.
71. Rutter M, Caspi A, Fergusson D et al. Sex differences in developmental reading disability: new findings from 4 epidemiological studies. JAMA 2004;**291**:2007–2012.
72. Retico A, Giuliano A, Tancredi R et al. The effect of gender on the neuroanatomy of children with autism spectrum disorders: a support vector machine case-control study. Mol Autism 2016;**7**:5.
73. Kim YK, Na KS. Application of machine learning classification for structural brain MRI in mood disorders: critical review from a clinical perspective. Prog Neuropsychopharmacol Biol Psychiatry 2017;**80**(Pt B):71–80.
74. Kassraian-Fard P, Matthis C, Balsters JH, Maathuis MH, Wenderoth N. Promises, pitfalls, and basic guidelines for applying machine learning classifiers to psychiatric imaging data, with autism as an example. Front Psychiatry 2016;**7**:177.
75. Orru G, Pettersson-Yeo W, Marquand AF, Sartori G, Mechelli A. Using support vector machine to identify imaging biomarkers of neurological and psychiatric disease: a critical review. Neurosci Biobehav Rev 2012;**2012**:1140–1152.
76. Halmoy A, Halleland H, Dramsdahl M, Bergsholm P, Fasmer OB, Haavik J. Bipolar symptoms in adult attention-deficit/hyperactivity disorder: a cross-sectional study of 510 clinically diagnosed patients and 417 population-based controls. J Clin Psychiatry 2010;**71**:48–57.
77. Asherson P, Young AH, Eich-Hochli D, Moran P, Porsdal V, Deberdt W. Differential diagnosis, comorbidity, and treatment of attention-deficit/hyperactivity disorder in relation to bipolar disorder or borderline personality disorder in adults. Curr Med Res Opin 2014;**30**:1657–1672.
78. Pereira F, Mitchell T, Botvinick M. Machine learning classifiers and fMRI: a tutorial overview. NeuroImage 2009;**45**:S199–S209.

79. Schnack HG, Kahn RS. Detecting neuroimaging biomarkers for psychiatric disorders: sample size matters. Front Psychiatry 2016;**7**:50.
80. Wang L, Wee CY, Tang X, Yap PT, Shen D. Multi-task feature selection via supervised canonical graph matching for diagnosis of autism spectrum disorder. Brain Imaging Behav 2016;**10**:33–40.
81. Wang J, Wang Q, Peng J et al. Multi-task diagnosis for autism spectrum disorders using multi-modality features: a multi-center study. Hum Brain Mapp 2017;**38**:3081–3097.

Supporting Information

Additional Supporting Information may be found in the online version of this article:

Figure S1. Spatial maps showing the pattern of GM regions used by the linear SVM classifier to discriminate between mixed-gender ADHD (n = 58) and HC (n = 58) subgroups.

Figure S2. Spatial maps showing the pattern of WM regions used by the linear SVM classifier to discriminate between mixed-gender ADHD (n = 58) and HC (n = 58) subgroups.

Figure S3. Spatial maps showing the pattern of FA regions used by the linear SVM classifier to discriminate between mixed-gender ADHD (n = 58) and HC (n = 58) subgroups.

Figure S4. Spatial maps showing the pattern of TR regions used by the linear SVM classifier to discriminate between mixed-gender ADHD (n = 58) and HC (n = 58) subgroups.

Figure S5. Spatial maps showing the pattern of GM regions used by the linear SVM classifier to discriminate between male-only ADHD (n = 52) and HC (n = 44) subgroups.

Figure S6. Spatial maps showing the pattern of WM regions used by the linear SVM classifier to discriminate between male-only ADHD (n = 52) and HC (n = 44) subgroups.

Figure S7. Spatial maps showing the pattern of FA regions used by the linear SVM classifier to discriminate between male-only ADHD (n = 52) and HC (n = 44) subgroups.

Figure S8. Spatial maps showing the pattern of TR regions used by the linear SVM classifier to discriminate between male-only ADHD (n = 52) and HC (n = 44) subgroups.

Appendix S1. Methods.

Table S1. Diagnostic performance of the GRBF kernel SVM classifier in the individual discrimination between mixed-gender ADHD (n = 58) and HC (n = 58) subgroups and between male-only ADHD (n = 52) and HC (n = 44) subgroups; using all features combinations.

Table S2. Diagnostic performance of the linear SVM classifier in the individual discrimination between mixed-gender ADHD (n = 58) and HC (n = 58) subgroups (n = 58) and between male-only ADHD (n = 52) and HC (n = 44) subgroups.

Table S3. Volumetric brain regions that best discriminated between mixed-gender ADHD (n = 58) and HC (n = 58) subgroups in the linear SVM classification.

Table S4. DTI regions that best discriminated between mixed-gender ADHD (n = 58) and HC (n = 58) subgroups in the linear SVM classification.